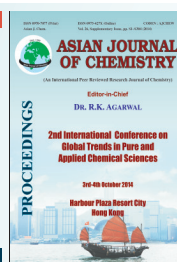


Asian Journal of Chemistry; Vol. 26, Supplementary Issue (2014), S291-S298

# ASIAN JOURNAL OF CHEMISTRY

<http://dx.doi.org/10.14233/ajchem.2014.19068>



## A Study of Poly-Ferric-Aluminum-Silicate-Sulfate: Preparation, Characterization and Application

WEI CHEN<sup>1,2</sup>, HUAILI ZHENG<sup>1,2,\*</sup>, YONGJUN SUN<sup>1,2</sup>, YUHAO ZHOU<sup>1,2</sup>, YUXIN ZHANG<sup>3</sup>,  
CHUN ZHAO<sup>1,2</sup>, XIAOMIN TANG<sup>1,2</sup>, JUN ZHAI<sup>1,2</sup> and WENWEN XUE<sup>1,2</sup>

<sup>1</sup>Key laboratory of the Three Gorges Reservoir Region's Eco-Environment, State Ministry of Education, Chongqing University, Chongqing 400045, P.R. China

<sup>2</sup>National Centre for International Research of Low-Carbon and Green Buildings, Chongqing University, Chongqing 400045, P.R. China

<sup>3</sup>College of Materials Science and Engineering, Chongqing University, Chongqing 400045, P.R. China

\*Corresponding author: Tel/Fax: +86 23 65120827; E-mail: zhl@cqu.edu.cn

Published online: 24 December 2014; AJC-16493

Coagulation-flocculation process is of great significance to water/wastewater treatment facilities. In this study, an effective composite coagulant poly-ferric-aluminum-silicate-sulfate was prepared with water glass,  $\text{FeSO}_4 \cdot 7\text{H}_2\text{O}$ ,  $\text{Al}_2(\text{SO}_4)_3 \cdot 18\text{H}_2\text{O}$  and  $\text{NaClO}_3$  as raw materials. Infrared spectra, scanning electron microscopy and Ferron analysis methods was adopted to characterize the poly-ferric-aluminum-silicate-sulfate under different  $\text{Si}/(\text{Fe}+\text{Al})$  and  $\text{OH}/(\text{Fe}+\text{Al})$  molar ratio. Coagulation behaviour of poly-ferric-aluminum-silicate-sulfate used in domestic wastewater treatment was extensively studied in a jar test by measuring turbidity, removal efficiency of chemical oxygen demand as well as zeta potential, sludge volume, flocs size ( $d_{50}$ ). The analysis of infrared spectra and scanning electron microscopy picture showed that the poly-ferric-aluminum-silicate-sulfate is a complex compound of Si and the metal ions. Ferron analysis results demonstrated that the species distribution of poly-ferric-aluminum-silicate-sulfate corresponded to  $\text{Si}/(\text{Fe}+\text{Al})$  and  $\text{OH}/(\text{Fe}+\text{Al})$  molar ratio at early aging stage, but the relationship was not well related with aging time. Coagulation experiment suggested that when  $\text{Si}/(\text{Fe}+\text{Al})$  was 1:9 and  $\text{OH}/(\text{Fe}+\text{Al})$  was 0.3, the coagulant exhibited superior water treatment performance. The optimal poly-ferric-aluminum-silicate-sulfate produced more sludge volume than polyaluminium silicate, but much less than other Fe-based coagulant. In addition, the coagulation mechanisms in water treatment process were found to be the adsorption/bridge formation and in a lesser extent, the adsorption/charge neutralization mechanism.

**Keywords:** Iron-based coagulant, Composite coagulant, Coagulation performance, Wastewater, Floc size.

### INTRODUCTION

The environmental problem caused by water pollution has posed a serious threat to human health<sup>1,2</sup>. Coagulation-flocculation process is an effective way to separate the impurities from water/wastewater with a wide range of applications in water treatment plant<sup>3</sup>. Coagulation-flocculation is a complex process including various mechanism as entrapment, adsorption/bridge-aggregation, sweep-flocculation charge neutralization, *etc.*<sup>4,5</sup>. The introduction of common coagulant as inorganic metal based substances neutralized the surface charge of suspended particles or colloidal systems and facilitated particle aggregation by absorption/sweep and settling under gravity as a result of electrical double layer compression.

Various materials have been developed for the purpose of coagulation/flocculation process in recent years. The point come into being from amount previous paper that coagulant/flocculant can be classified into inorganic-based, organic-based

as well as hybrid materials. Among them inorganic coagulant refer to metal-based coagulant, such that Fe-based, Al-based and Ti-based, *etc.*, which were low-cost, superior coagulation performance and has been used for hundreds years<sup>6,7</sup>. While organic flocculant was defined as three or more organic monomer units reacted together to synthetic long chain organic compounds. However, due to the link between aluminum and neuropathological diseases such as Alzheimer's disease<sup>8</sup>, while the effluent of iron-based coagulation system usually has higher chromaticity colour and corrosivity, which limit the development of metal-based coagulants. Composite coagulant used in coagulation/flocculation process of wastewater are materials obtained from the addition of effective components into the original material to enhance the aggregating power. Composite materials thus have emerged as new materials that pose tremendous potential in treating wastewater due to their better performance than that of metal-based coagulant and its lower cost than that of organic-based flocculants.

Composite product have been received wide spread attention in recent decades<sup>6,9,10</sup>. Gao *et al.*<sup>11</sup> developed a type of composite inorganic polymer coagulant, poly-aluminum-silicate-chloride, the results shows that some interactions have been discovered between hydrolyzed aluminum species and polysilicic acid and PASiC is better than PAC in coagulation performance. Wang *et al.*<sup>9</sup> prepared a composite flocculants from iron salts and polydimethyl-diallylammonium chloride (PDMDAAC), the paper demonstrated that when PDMDAAC fraction (Wp) was 7 %, PFC-PDMDAAC contained the smallest content of  $Fe_c$  and had the highest zeta potential. Beaker stirring experiment showed PFC-PDMDAAC produced the highest flocculation efficiency compared with that of  $FeCl_3$ , PFC and PDMDAAC. Sun *et al.*<sup>12</sup> prepared poly-ferric-aluminum-silicate-sulfate (PFASS) with various (Al+Fe)/Si, the character results revealed that 16:1 (Al+Fe)/Si molar ratio is favor to forming of Si-O-Al and Si-O-Fe bonds, the coagulation behaviour of PFASS showed the optimal (Al+Fe)/Si molar ratio for the turbidity and chemical oxygen demand removal is different, 12:1 and 16:1, respectively.

Ferric-based coagulant prepared with polysilica acid is a new composite coagulant and drew widespread investigation in recent years<sup>12-14</sup>. The research paper shows Fe-Si-based coagulant can be prepared from industrial wastes, oil shale ash and other low cost raw material. Compared with other PSF coagulants at the same dosage in jar test, PFSS exhibits better coagulation performance, especially in UV<sub>254</sub>, chemical oxygen demand, turbidity removal efficiency, *etc.*<sup>12,14,15</sup>. But it is obvious that the great gap among the comprehension research about the coagulation performance of PFASS have not been fulfilled perfectly. In this paper, PFASS was prepared by hydroxylation of the mixture consisting of  $Fe_2(SO_4)_3$  and fresh polysilicic acid using ferrous sulfate ( $FeSO_4 \cdot 7H_2O$ ), aluminum sulfate [ $Al_2(SO_4)_3$ ] and sodium silicate ( $Na_2SiO_3$ ) as raw materials.

The possible chemical bonds and the morphology of PAFS were observed using Fourier transformed infrared (FT-IR) spectrophotometer and scanning electron microscopy (SEM). The aqueous Fe-Al species was measured by ferron complexation timed spectrophotometric method under different Si/(Al+Fe) and OH/(Al+Fe). Following, the paper focus on exploring the effect of various Si/(Al+Fe) molar ratio on the turbidity, chemical oxygen demand and zeta potential changes as well as Fe-Al species, sludge volume and floc size. Lastly, the paper shed light upon the coagulation/flocculation mechanism through which the removal of impurity takes place.

## EXPERIMENTAL

The main agents and it's information were listed in Table- 1.

The instruments adopted in the experimental setup were as follows: Fourier transformed infrared: IR Prestiger-21, Japan. Scanning electron microscope (SEM): Vega II LMU, Czech Republic; ZR4-6 Jar Tester: Zhongrun Water Industry Technology Development Co. Ltd. Shenzhen, China; Particle size and zeta potential analyzer: Zetasizer Nano ZS90, Britain; Chemical oxygen demand analyzer: DR2008, USA; Turbidity meter: HACH 2100Q, USA.

The raw water used in this study was collected from the sewer system of Chongqing University. The wastewater sample was filtered using 400 micromesh sieve to remove large particles and the sample was characterized in terms of the concentrations of turbidity, chemical oxygen demand and pH, the value of which were 90-130 NTU, 140-185 mg/L and 7.82-8.4, respectively.

**Preparation of coagulant:** The preparation methods of poly silicic acid is the same as Xu *et al.*<sup>16</sup>.

The water glass was diluted to 3 % (m/m) with deionized water, then introduced into sulfuric acid solution (20 % m/m) slowly while stirring with magnetic stirring apparatus at room temperature (25 °C), the pH of which was regulated  $3 \pm 0.2$  by 0.5 M  $H_2SO_4$  and 1 M NaOH. After that, the silicic acid solution was kept quietly and aged for around 1 h to get good polymerization.

40 g of  $FeSO_4 \cdot 7H_2O$  was dissolved in 33 mL 20 %  $H_2SO_4$  solution under slow stirring in a beaker until a homogeneous ferrous sulfate liquid mixture was obtained at room temperature. The temperature of which was controlled by a thermostatic water bath. 2.6 g of  $NaClO_3$  was added into the reaction vessel as oxidizing agent to oxidate the Fe(II) in the pickle liquor to Fe(III). Then, the  $Al_2(SO_4)_3 \cdot 18H_2O$  was mixed with  $Fe_2(SO_4)_3$  solution according to different Al/Fe molar ratios ranging from 6:4 to 1:9, resulting in the formation of a new liquid mixture. The new solution mixture was stirred for 10 min in a thermostatic water bath at a pre-determined temperature.

The silicic acid solution was added into metal salt solution at slow speed under stirring, after the addition of silicic acid for 10 min,  $NaHCO_3$  powder was added into the above solution to obtain the desired  $\gamma$  value ( $\gamma = OH/Fe$  molar ratio) ranging from 0.1 to 0.6. After keeping stirring for 60 min in a thermostatic water bath, the reaction mixture was stored at room temperature 24 h for further polymerization and aging.

**Structure, morphology and ferron analysis:** The samples of liquid coagulants were dried in a vacuum at 60 °C for several days and ground into powders, which were measured by a fourier transformed infrared (FT-IR) spectrophotometer to get

TABLE-1  
MAIN AGENTS USED IN THE EXPERIMENT

Reagent	Grade	Supplier
Ferrous sulfate ( $FeSO_4 \cdot 7H_2O$ )	Technical grade	Chongqing Lanjie Tap Water Company (Chongqing, China)
Aluminum sulfate ( $Al_2(SO_4)_3$ )	Analytical grade	Chengdu Kelong Chemical Reagent Company (Chengdu, China)
Water glass	Industry grade, $w(SiO_2) = 26 \%$	College of civil engineering, Chongqing university
Sulfuric acid ( $H_2SO_4$ )	Analytical grade	Chongqing Lanjie Tap Water Company (Chongqing, China)
Sodium chlorate ( $NaClO_3$ )	Analytical grade	Sinopharm Chemical Reagent Co., Ltd (Shanghai, China)
De-ionized water	Conductivity $\leq 0.51$ S/cm	Chongqing University (Chongqing, China)

the FT-IR characteristic peaks of PFASS. The spectrum was measured in the range of 4000-400  $\text{cm}^{-1}$ . Latter, the morphology of the coagulants were examined using a scanning electron microscope (SEM).

In the coagulant mixture solution, owing to different extent of hydrolysis and polymerization, Fe-Al species can be artificially divided into three kind,  $(\text{Fe-Al})_a$ ,  $(\text{Fe-Al})_b$  and  $(\text{Fe-Al})_c$ .  $(\text{Fe-Al})_a$  species represent the free ion and mononuclear hydroxyl complex, while  $(\text{Fe-Al})_b$  species were defined as the formation of many poly-nuclear complexes,  $(\text{Fe-Al})_c$  species were regard as the complexes of high molecular polymer and  $\text{Fe}(\text{OH})_3$ . For the purpose of classifying the suspension Fe-Al species, the ferron-complexation timed spectrophotometric method was adopt based on the standard adsorption curves of the reaction between poly-aluminum-ferric-silicate and the ferron reagent (8-hydroxy-7-iodoquinoline-5-sulphonic acid). Visible light absorbance was measured as a function of time at a wavelength of 597 nm to quantify the amount of Fe complex. The absorbance observed within the first minute. of the liquor ascribed to the  $(\text{Fe-Al})_a$ , after 4 h, the absorbance finally ended in a plateau, the absorbance corresponded to the  $(\text{Fe-Al})_a$  and  $(\text{Fe-Al})_b$  species; while after boiling for 0.5 h, the absorbance was marked as unread the  $(\text{Fe-Al})_c$ .  $(\text{Fe-Al})_c$  values were calculated by subtracting  $(\text{Fe-Al})_a$  and  $(\text{Fe-Al})_b$  from the  $(\text{Fe-Al})_c$ . The more detailed experiments method was based on the paper studied by Dong *et al.*<sup>17</sup>.

**Flocculation test:** Coagulation-flocculation test were performed in six 1-L plexiglas beaker using a programmable jar-test apparatus at room temperature. One liter of wastewater sample was poured into a beaker and the initial pH was adjusted to set value using 0.5 M NaOH and HCl. During each experiment, the coagulation process composed of a rapid agitation stage at 250 rpm for 1 min to obtain homogeneous dispersion, followed by a slow agitation stage at 40 rpm for 10 min and then a step of sedimentation for 0.5 h. A certain dosage of coagulant was added at the start of the first agitation step. The supernatant sample was extracted from the beaker 3 cm below the water surface for further analysis, each run was performed triplicate and the value is the means of two most resemble.

Zeta potential of the dispersion suspension was measured using a Zetasizer 3000 Hsa, which was collected in water sample as soon as rapid agitation stage finished. Turbidity of the supernatant water was tested measurement using a model turbidimeter. Chemical oxygen demand was also tested using a HACH chemical oxygen demand reactor and expressed as  $\text{COD}_{\text{Cr}}$  (potassium dichromate as oxidant). The floc size of sludge which precipitated in the bottom of the beaker was measured simultaneously by Winner 2000 laser particle size analyzer.

## RESULTS AND DISCUSSION

**FT-IR spectroscopy:** Fig. 1 present the FT-IR spectroscopy for PFS and PFASS. By checking the FT-IR characteristic peaks in the range of 4000-400  $\text{cm}^{-1}$  and matching the corresponding chemical bonds, the possible chemical bonds in PFS and PFASS can be obtained. As showed in Fig. 1 that there is a broad absorption peak in the range of 3250-3500  $\text{cm}^{-1}$  for both PAFS and PFS (3416  $\text{cm}^{-1}$  for PFS and 3393

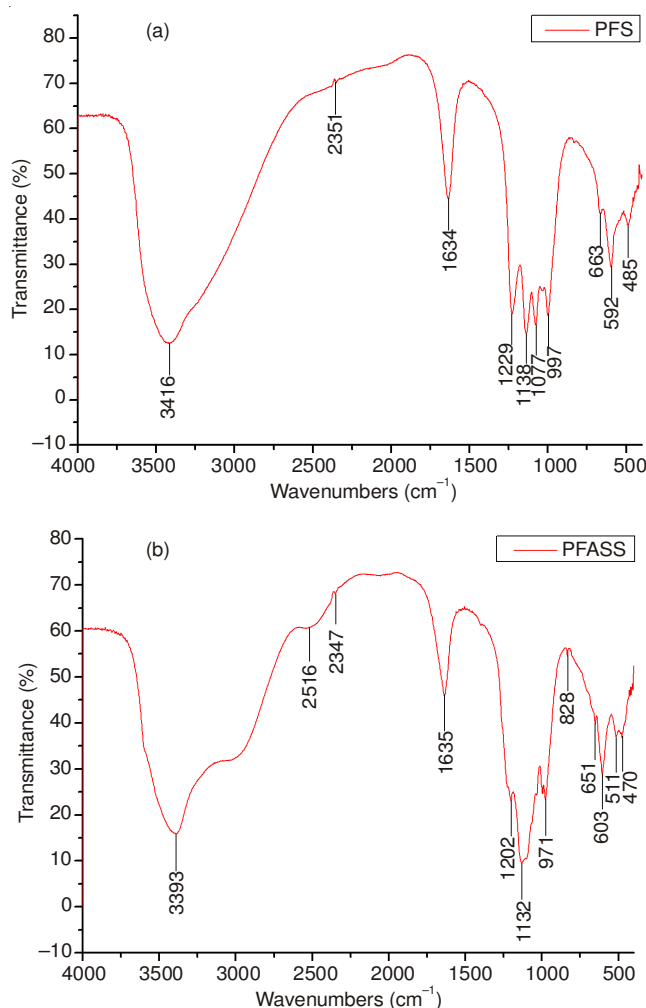


Fig. 1. FT-IR spectra for (a) PFS and (b) PFASS

$\text{cm}^{-1}$  for PFS), which can be interpreted as the intermolecular association stretching vibration of -OH, while the intensity of the above peak in PFS is stronger than PAFS. Furthermore, the peak at 2516  $\text{cm}^{-1}$  for PAFS is related to the intermolecular chelation vibration of -OH, which are weak or disappeared in the infrared spectra of PFS<sup>7,18</sup>. The medium peak in the range of 1650-1600  $\text{cm}^{-1}$  (1634  $\text{cm}^{-1}$  for PFS and 1635  $\text{cm}^{-1}$  for PFASS), was attributed to the bending vibration of the water absorbed, polymerized and crystallized in the coagulant. The different intensities of the above peaks between two products implied that the introducing of Al and Si into PAS changed the amount of -OH and H-O-H in the coagulant, while -OH group plays an important role in coagulation progress<sup>19</sup>. There is large absorption peaks around 1130-1230  $\text{cm}^{-1}$ , which is based on the asymmetric stretching vibration of Fe-OH-Fe or Al-OH-Al, besides the infrared spectra spectral studies revealed that the characteristic absorption peak for Fe-O-Fe or Al-O-Al was evident in the range of 1077  $\text{cm}^{-1}$ . The wave number of Fe-OH-Fe is larger than Fe-O-Fe and PFASS shows hypsochromic shifts of Fe-O-Fe, which is assigned to the addition of Al and Si lead to the copolymerization between materials. In addition, there was a strong adsorption peak at 997  $\text{cm}^{-1}$  in Fig. 1a, which could be assigned to the  $\text{SO}_4^{2-}$  stretching vibration, while in Fig. 1b, adsorption peak around 997  $\text{cm}^{-1}$  is weak, or even disappear. Meanwhile, the characteristic peak of 971  $\text{cm}^{-1}$  is



assigned to Si-O-Fe or Si-O-Al, which is absent in PFS, these bonds hydrolyzed during coagulation process and produce a hydroxy complex with mono-core or multicore silicon and the poly-silicon fragment with Fe or Al is favorable for coagulation-flocculation performance. Whereas the peaks at the range of  $670\text{--}470\text{ cm}^{-1}$  are assigned to the stretch vibration of Fe-O or Al-O bonds and the bending vibrations of Fe-OH and Al-OH. The FT-IR spectroscopy study result provide the evidence that the product is not a simple mixture of raw materials but a complex compound by iron, aluminum and silicon.

**Scanning electron microscopy analysis:** The possible chemical bonds were investigated by the FT-IR while the morphology was observed by the scanning electron microscopy.

As studied in previously papers, the spherical and spheroidal partical morphology of PS and the cross-copolymerization between Fe, Al and Si in PFASS coagulant, the introduction of PS and Al into PFS would change the surface morphology and structure of coagulants obviously<sup>16,19,20</sup>. Fig. 2a shows the morphology of PFS slices are thick, long, tube-like shape, unlike those observed in Fig. 2b, but the conclusions were drawn based on previous studies showed that branched structure is beneficial to coagulate colloidal particles form bridge-aggregation among flocs in coagulation process. Furthermore, in long storage time, PFS would degenerate into solid sediment<sup>21</sup> for the hydrolyzation of  $\text{Fe}^{3+}$ . In order to improve the case of hydrolyzation, introducing other materials as stabilizer into the product is necessary. In this study, silicic acid and  $\text{Al}_2(\text{SO}_4)_3$  was added into the solution as stabilizer. Fig. 2b shows the morphology of PFASS under the superior prepare condition. Branch-like or even network structures can be observed in the photograph. The unique morphologies are horizontally made up of small irregular units, which are fit for the adsorption and aggregation of fine particles. The beaker

experiments reveals that PFASS is superior in stability and coagulation performance. Fig. 2 also shows the degree of linear correlation projected area (A) and the characteristic length (L). As illustrated in calculation for two dimensional fractal dimension using Image-Pro Plus 6.0 software, the average fractal dimensions of PFS and PFASS were 1.40 and 1.46, respectively.

**Effect of Si/(Fe+Al) on coagulation/flocculation performance:** Beaker experiments were adopt to examine the coagulation efficiency of six coagulant, PFASS7 (PFASS7 represent  $\text{Si}/(\text{Al}+\text{Fe}) = 1:7$ , by that analogy in the following), PFASS9, PFASS12, PFASS16, PFS and PAS comprehensively. The evaluation index of coagulation performance is turbidity removal efficiency, chemical oxygen demand removal efficiency, the change of zeta potential, sludge volume, sludge particle size et, which is of great significant in practical engineering application.

**Effect of coagulants on the change of turbidity, chemical oxygen demand and zeta potential:** The Al/Fe and OH/Fe of PFASS coagulant used in the study is of 3/7, 0.3, respectively. While the basicity of PAS or PFS is the same as PFASS [ $\text{OH}/(\text{Al}+\text{Fe}) = 0.3$ ].

Fig. 3a shows the turbidity removal efficiency changed with the increasing of coagulant dosage. The diagram illustrated that the distinction between six coagulant in turbidity removal is minor, when the dose below 1 mmol/L, the removal efficiency increased rapidly with the addition of coagulant, When the coagulant dosage was in the range of 1–4 mmol/L, the efficiency presented a slighter rise as the dosage increased. Whereas as the coagulant dosage increased further, the removal efficiency decreased. The chemical oxygen demand removal efficiencies manifested the same tendency (Figs. 3b and 3c) showed that zeta potential continuously increased with the dosage and remained blow 0 mV within the dosage selected

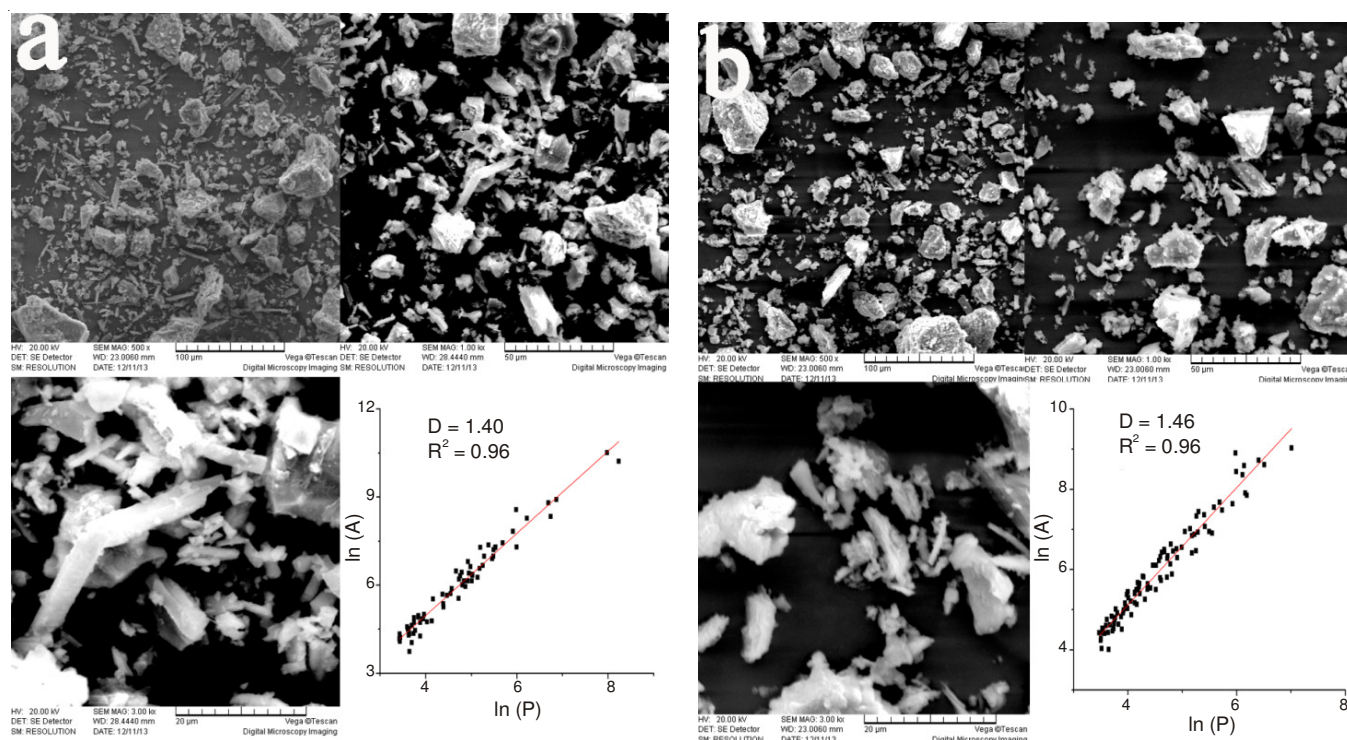


Fig. 2. SEM photographs for (a) PFS and (b) PFASS

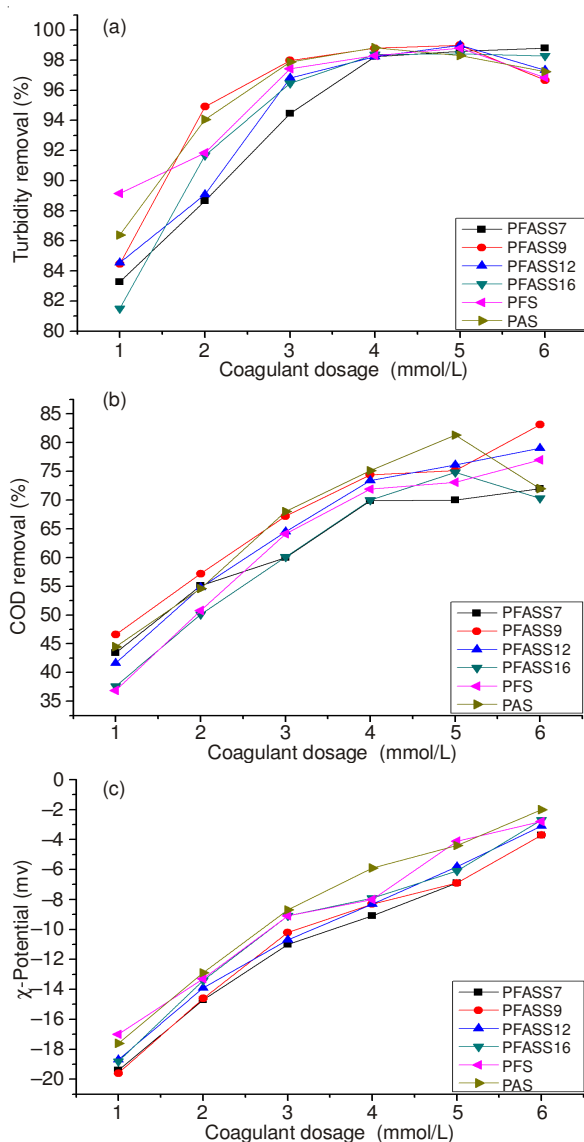


Fig. 3. Effect of types of coagulants on turbidity, chemical oxygen demand removal efficiency and zeta potential change

in this study. Which demonstrate that the zeta potential increased sharply first and then smoothly in each product. However, PFS and PAS exhibits higher zeta potential for each applied coagulant dosage, which displayed that the introduction of silica acid would weak the coagulant's absorption/charge neutralization ability<sup>22,23</sup>. The changes in the zeta potential values of colloid particles are generally used to evaluate the destabilization ability of coagulation reagents. While, previous studies have demonstrated that the predominant mechanism is charge neutralization, entrapment and adsorption<sup>16,24,25</sup>. The zeta potential blow 0 mv indicated that the predominant coagulation mechanism is the adsorption/bridge formation and in a lesser extent, the adsorption/charge neutralization mechanism.

The removal efficiency of turbidity and chemical oxygen demand increased sharply within the dosage range 0 and 1 mmol/L, to around 85, 40 %, respectively. The higher impurity removal efficiency can be attributed to as soon as coagulant dose, the quickly hydrolysis of metal ion into larger particles colloidal as  $\text{Al}_2(\text{OH})_2^{4+}$ ,  $\text{Al}_3(\text{OH})_4^{5+}$ ,  $\text{Al}_{13}\text{O}_4(\text{OH})_{24}^{7+}$ ,  $\text{Fe}_2(\text{OH})_2^{4+}$ ,  $\text{Fe}_3(\text{OH})_4^{5+}$ , and the polymer could adsorb onto the surface of the larger colloids in water its long-chains where the tails and loops are extended far beyond its surface and can interact with other particles *via* bridging flocculation<sup>1,6,26</sup>. Compared with six coagulant, PFASS9 [Si/(Al+Fe) = 1:9] and PAS exhibit superior turbidity and chemical oxygen demand removal efficiency at whole dosage range. Aluminium-based coagulants shows excellent impurity removal performance and have been used for hundreds years<sup>27</sup>. However, concerns have been raised about the potential toxicity of residual aluminum and therefore, a threat to human health and the environment<sup>28</sup>, which inhibit the large-scale applications of aluminium-based coagulants in water/wastewater treatment. The optimal dosage in this study is 5 mmol/L, in more case, removal efficiency increased with the addition of coagulant blow 5 mmol/L and decreased above 5 mmol/L, yet. The distinction of four poly-ferric-aluminum-silicate-sulfate is the amount of polysilicic acid introduced into products. The proper addition of polysilicic acid into the structure of the coagulants would improves their coagulation performance by providing a coagulation agent with increased molecular size and enhanced aggregating power, thus the particle in solution can be swept away *via* the "adsorption and charge neutralisation" mechanisms<sup>29</sup>. The presence of silica facilitate the polymerization process between polysilica and metal ion through Al-O-Si or Fe-O-Si bond, which enhances the coagulation efficiency, as it facilitates the formation of large and better settleable flocs, through the adsorption/bridge formation mechanism<sup>30</sup>. Whereas, the excessive proportion of silica turn out to be unbeneficial to coagulation performance, for negatively charged polysilica acid would weaken the absorption/charge neutrality ability of coagulants, furthermore, as displayed in Table-2, too much polysilica is bad for the polymerization process of metal ion coagulant.

Table-2 illustrates the speciation of all samples which was conducted after 72 h aging. The different species of Fe-Al can be classified into three categories, *i.e.* as  $(\text{Fe-Al})_a$  (oligomers),  $(\text{Fe-Al})_b$  (polymers) and  $(\text{Fe-Al})_c$  (precipitated species). As showed in Table-2, the species distribution of PFASS is strictly correspond to different Si/[Al+Fe], the amount of  $(\text{Fe-Al})_a$  and  $(\text{Fe-Al})_b$  increased with the addition of polysilica, which demonstrated that Si/(Fe+Al) molar ratios show some effect on the degree of polymerization<sup>15</sup>. As stated earlier,  $(\text{Fe-Al})_b$  is the predominant species in coagulation, the beaker stirring experiment is accordance with the conclusion perfectly.

**Effect of coagulants on the sludge volume:** Sludge volume and sludge moisture content is a great significance

TABLE-2  
Fe-Al SPECIES DISTRIBUTION OF PAFSS WITH DIFFERENT Si/(Fe+Al) MOLAR RATIOS

Al/Fe molar ratio	PFASS7	PFASS9	PFASS12	PFASS16	PFS
$(\text{Fe-Al})_a$	0.69	0.56	0.58	0.31	0.18
$(\text{Fe-Al})_b$	0.19	0.24	0.18	0.42	0.07
$(\text{Fe-Al})_c$	0.12	0.20	0.24	0.27	0.75

index in water/wastewater treatment plant, for the huge production of waste sludge and its potential pollution may pose a serious environmental problem to our society. Fig. 4. displays the effect of types of flocculants on sludge volume. From the graph we can know that PFASS9 produced fewer sludge volume compared to four Fe-coagulant, while PFS exhibit opposite result. The sludge volume reduced with the increase of Si/(Al+Fe), the consequence probable suggest that at lower Si/(Al+Fe) molar ratio, the better chain-net structure of PFASS lead to stronger absorption bridging ability. Instead, at higher Si/(Al+Fe) molar ratio, exceeded silicon results in chain-net structure of PFASS destroyed and then the absorption bridge ability is lower than before<sup>12</sup>. Overall consideration the effect of Si/(Al+Fe) on coagulation-flocculation efficiency, Si/(Al+Fe) = 1:9 shows better integrated performance.

**Effect of coagulants on the floc size distribution:** Fig. 5 illustrates the results of floc size of different coagulants measured

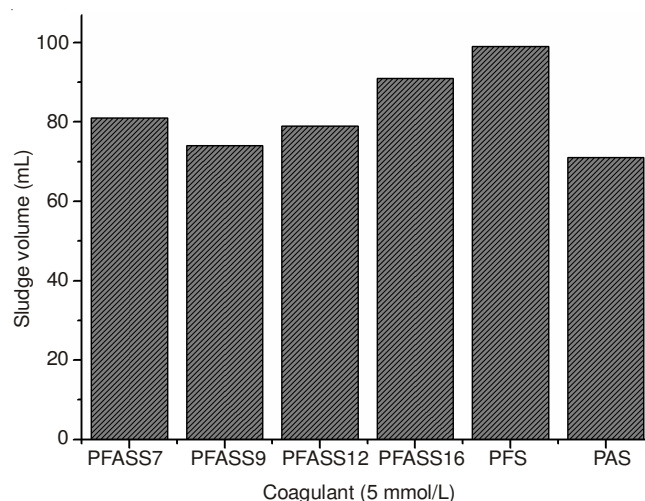


Fig. 4. Effect of types of flocculants on sludge volume

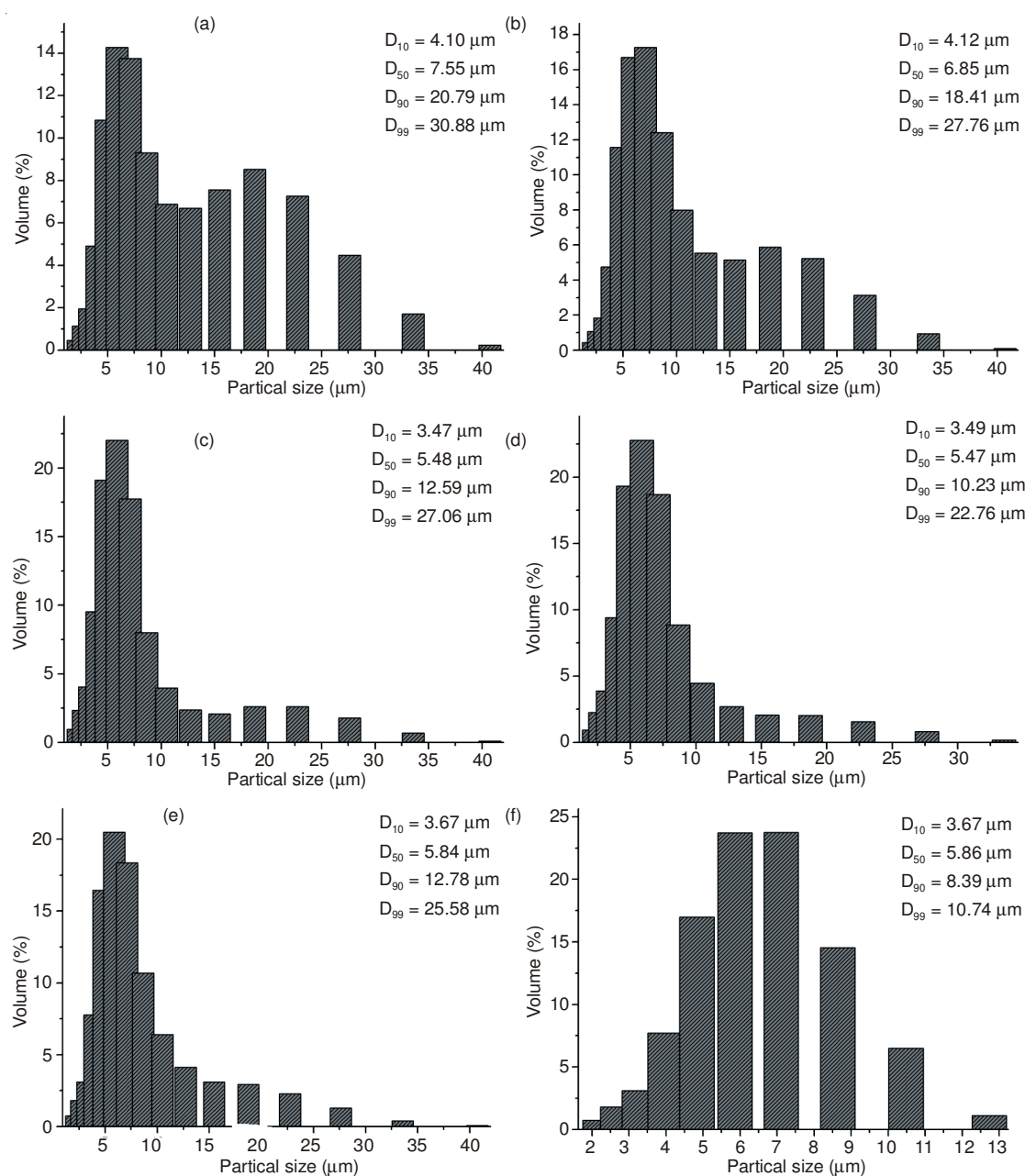


Fig. 5. Effect of coagulants on the floc size distribution. a. PFASS7, b. PFASS9, c. PFASS12, d. PFASS16, e. PFS, f. PAS



by Winner 2000 laser particle size analyzer, which were noted as the respective particle sizes corresponding to 10, 50, 90 and 99 % of the size histogram. While  $D_{10}$  represent the floc size that 10 % of flocs were in the range of  $[0 \mu\text{m}-D_{10}]$ . Similarly,  $D_{50}$  means 10 % of flocs were in the range of  $[0 \mu\text{m}-D_{50}]$  and so on. Since larger flocs are apt to sediment and resist to flow turbulence, which are the advantage in the coagulation/flocculation progress<sup>30,31</sup>.

Fig. 5. displays the floc size distribution at the end of flocculation process for a. PFASS7, b. PFASS9, c. PFASS12, d. PFASS16, e. PFS and f. PAS. The median equivalent volumetric diameter selected as the relative floc size was  $d_{50}$ , although the same trends were observed for the whole range of floc size investigated. In the studies, the size was measured at the optimal coagulant dosage of 5 mmol/L. It can be learn from the picture that the value of six coagulants is 7.55  $\mu\text{m}$  for PFASS7, 6.85  $\mu\text{m}$  for PFASS9, 5.48  $\mu\text{m}$  for PFASS12, 5.47  $\mu\text{m}$  for PFASS16, 5.84  $\mu\text{m}$  for PFS, 5.86  $\mu\text{m}$  for PAS and the order of  $d_{50}$  of six coagulant is as follows: PFASS7 > PFASS9 > PAS > PFS > PFASS12 > PFASS16. According to the previous studies, the enlargement of floc size was thought to have positive effect on the colloid/particle removal<sup>32</sup>. The conclusion can be drawn that the floc size has significant positive correlation with the Si/(Fe+Al) molar ratio. Previous study have shown higher Si/(Al+Fe) molar ratio exhibits better coagulation performance, the introduction of polysilica acid would enhance coagulant's neutralization, adsorption and capture capacities and results in the formation of large polymeric chains with high molecular weight<sup>15</sup>.

**Effect of OH/(Fe+Al) on coagulation/flocculation performance:** Basicity is a significant parameter affecting the product's coagulation behaviour. Too low OH/(Fe+Al) is unfavourable for the degree of polymerization, thus lead to weak absorption/bridge and aggregation ability in the coagulation/flocculation process. Whereas, higher OH/(Fe+Al) is not good for the aging of products, for higher basicity would accelerate the hydrolysis of metal ion and the appears of sedimentation decreased the effective constitute of the coagulants<sup>33</sup>. Furthermore, pH value is a crucial factor affecting the gelation of polysilica acid, which would reduce the coagulation efficiency as well<sup>29</sup>. For proper alkalinity degree is essential to superior coagulant products.

Fig. 6a shows the turbidity and chemical oxygen demand removal efficiency varies with the different of OH/(Fe+Al) at the aging time of 24 h. The conclusion can be drawn from the data that at the range of 0.2-0.5 OH/(Fe+Al), turbidity removal efficiency enhanced with the increase of the OH/(Fe+Al), while chemical oxygen demand removal efficiency showed similar trend as well. However, as illustrated in Fig. 6b, the aging time of 72 h, the optimal OH/[Fe+Al] molar ratio is 0.3, the coagulation efficiency decreased with more alkali. Fig. 6c display the pH and zeta potential varies with the different basicity. The pH varies around 6.7 to 6.8, but the pH declined in OH/(Fe+Al) = 0.7 indicate the weak relation between coagulants basicity and treated water sample. The zeta potential decreased with the increasement of OH/(Fe+Al) molar ratio, which imply that the absorption/charge neutralization ability would deteriorate with higher basicity.

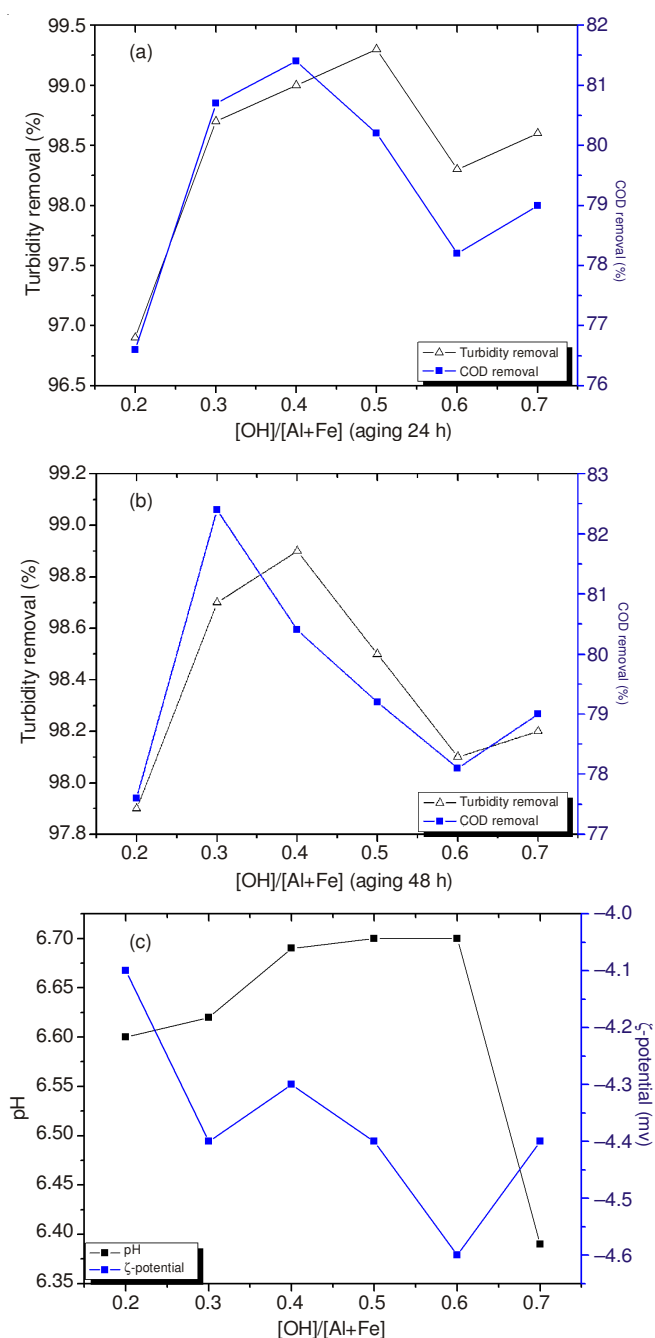


Fig. 6. Effect of OH/[Fe+Al] and aging time on turbidity, COD and zeta potential change

Table-3 illustrates the speciation of all samples in different OH/[Fe+Al] which was conducted after 24 and 72 h aging. The data shows that the amount of  $\text{NaHCO}_3$  introduced have significant effect on the species distribution of PFASS corresponding with OH/[Fe+Al] ratio at the aging time of 24 h. While in 72 h the species distribution of PFASS is not corresponding strictly with OH/[Fe+Al] ratio, the results demonstrate the preparation OH/[Fe+Al] has little effect on the species distribution. According to previous report, increasing the content of the  $(\text{Fe-Al})_b$  species would lead to an increase in the flocculation efficiency<sup>19</sup>. However, at high content of the  $(\text{Fe-Al})_c$  species, the coagulation-flocculation performance would decrease. The jar test discussed above suggest that higher or

TABLE-3  
Fe-Al SPECIES DISTRIBUTION OF PAFSS WITH DIFFERENT OH/[Fe+Al] MOLAR RATIOS AND AGING TIME

OH [Fe+Al]	0.2	0.3	0.4	0.5	0.6
(Fe-Al) <sub>a</sub> 24 h	0.81	0.76	0.68	0.51	0.39
(Fe-Al) <sub>b</sub> 24 h	0.01	0.04	0.02	0.07	0.08
(Fe-Al) <sub>c</sub> 24 h	0.17	0.21	0.30	0.41	0.53
(Fe-Al) <sub>a</sub> 72 h	0.53	0.47	0.36	0.44	0.43
(Fe-Al) <sub>b</sub> 72 h	0.06	0.09	0.04	0.07	0.06
(Fe-Al) <sub>c</sub> 72 h	0.41	0.44	0.60	0.49	0.52

lower basicity has a negative effect on coagulation efficiency. In addition, OH/[Fe+Al] around 0.3 or 0.4 is beneficial to coagulation-flocculation performance, OH/[Fe+Al] = 0.3 is adopt as an significance parameter to synthesis the coagulant.

### Conclusions

In this study, the structure, morphology, species distribution and coagulation performance of composite coagulant PFASS were investigated, the main conclusion drawn from the were list as following:

(i) FT-IR spectroscopy analysis shows that the new chemical bonds as Si-O-Fe, Si-O-Al or Fe-OH-Fe was generated in the preparation process. Scanning electron microscopy analysis manifest the average fractal dimensions of PFS and PFASS were 1.40 and 1.46, respectively.

(ii) Beaker experiment demonstrate that coagulant performed superior turbidity and chemical oxygen demand removal efficiency when Si/(Al+Fe) = 1:7, in this preparation condition, coagulation test performed fewer sludge volume and larger flocs size ( $d_{50}$ ). The result suggests the predominant mechanism maybe sweep, entrapment and interparticle bridging and in less extent, adsorption/bridge neutrality.

(iii) Ferron analysis indicated the species distribution of PFASS corresponding with OH/[Fe+Al] ratio at the aging time of 24 h. While in 72 h aging time suggest the amount of NaHCO<sub>3</sub> addition in the range of OH/[Fe+Al] 0.2-0.7 has little effect on the species distribution. Coagulation/flocculation experiment implied coagulant performed perfect turbidity and chemical oxygen demand removal efficiency at OH/[Fe+Al] = 0.7.

### ACKNOWLEDGEMENTS

The research was supported by the Central University Basic Scientific Research Foundation of Building division at Chongqing University (No. 106112014CDJZR210004).

### REFERENCES

1. A. Azizullah, M. N. K. Khattak, P. Richter, and D. Häder, *Environ. Int.*, **37**, 479 (2011).
2. B. Wei and L. Yang, *Microchem. J.*, **94**, 99 (2010).
3. J. Wei, B. Gao, Q. Yue, Y. Wang, W. Li and X. Zhu, *Water Res.*, **43**, 724 (2009).
4. Y. Fu, S. Yu and C. Han, *Chem. Eng. J.*, **149**, 1 (2009).
5. P. Jarvis, E. Sharp, M. Pidou, R. Molinder, S.A. Parsons and B. Jefferson, *Water Res.*, **46**, 4179 (2012).
6. K.E. Lee, N. Morad, T.T. Teng and B.T. Poh, *Chem. Eng. J.*, **203**, 370 (2012).
7. Y. Zeng and J. Park, *Colloids Surf. A*, **334**, 147 (2009).
8. J. Guo, D. Jiang, Y. Wu, P. Zhou and Y. Lan, *J. Hazard. Mater.*, **194**, 290 (2011).
9. Y. Wang, B. Gao, Q. Yue, J. Wei and Q. Li, *Chem. Eng. J.*, **142**, 175 (2008).
10. B.-Y. Gao, Y. Wang, Q.-Y. Yue, J.-C. Wei and Q. Li, *Sep. Purif. Technol.*, **62**, 544 (2008).
11. B.Y. Gao, Q.Y. Yue, B.J. Wang and Y.B. Chu, *Colloids Surf. A*, **229**, 121 (2003).
12. T. Sun, L. Liu, L. Wan and Y.-P. Zhang, *Chem. Eng. J.*, **163**, 48 (2010).
13. C. Sun, Q. Yue, B. Gao, B. Cao, R. Mu and Z. Zhang, *Chem. Eng. J.*, **185-186**, 29 (2012).
14. Y. Fu and S.L. Yu, *J. Non-Cryst. Solids*, **353**, 2206 (2007).
15. P.A. Moussas and A.I. Zouboulis, *Sep. Purif. Technol.*, **63**, 475 (2008).
16. X. Xu, S. Yu, W. Shi, Z. Jiang and C. Wu, *Sep. Purif. Technol.*, **66**, 486 (2009).
17. H. Dong, B. Gao, Q. Yue, H. Rong, S. Sun and S. Zhao, *Desalination*, **335**, 102 (2014).
18. P.A. Moussas and A.I. Zouboulis, *Water Res.*, **43**, 3511 (2009).
19. G. Zhu, H. Zheng, Z. Zhang, T. Tshukudu, P. Zhang and X. Xiang, *Chem. Eng. J.*, **178**, 50 (2011).
20. H. Zheng and G. Zhu, S. Jiang, T. Tshukudu, X. Xiang, P. Zhang and Q. He, *Desalination*, **269**, 148 (2011).
21. J. Dousma and P.L. de Bruyn, *J. Colloid Interf. Sci.*, **64**, 154 (1978).
22. M. Dietzel, *Geochim. Cosmochim. Acta*, **64**, 3275 (2000).
23. B.-Y. Gao, Q.-Y. Yue and Y. Wang, *Sep. Purif. Technol.*, **56**, 225 (2007).
24. N.D. Tzoupanos, A.I. Zouboulis and C.A. Tsoleridis, *Colloids Surf. A*, **342**, 30 (2009).
25. B. Gao, H. Hahn and E. Hoffmann, *Water Res.*, **36**, 3573 (2002).
26. R. Li, C. He and Y. He, *Desalination*, **319**, 85 (2013).
27. J. Duan and J. Gregory, *Adv. Colloid Interface Sci.*, **100-102**, 475 (2003).
28. J.L. Lin, C. Huang, J.R. Pan and D. Wang, *Chemosphere*, **72**, 189 (2008).
29. A.I. Zouboulis and P.A. Moussas, *Desalination*, **224**, 307 (2008).
30. D. Wang and H. Tang, *Water Res.*, **35**, 3418 (2001).
31. C. Wu, Y. Wang, B. Gao, Y. Zhao and Q. Yue, *Sep. Purif. Technol.*, **95**, 180 (2012).
32. S. Biggs, M. Habgood, G.J. Jameson and Y.- Yan, *Chem. Eng. J.*, **80**, 13 (2000).
33. S. Kratochvil and E. Matijevic, *J. Colloid Interf. Sci.*, **24**, 47 (1967).